DRFC/CAD

EUR CEA-FC-1472

ADJOINT OPTIMIZATION SCHEME FOR LOWER HYBRID CURRENT RAMPUP AND PROFILE CONTROL IN TOKAMAKS

X. Litaudon, D. Moreau, J. P. Bizarro, G. T. Hoang, K. Kupfer, Y. Peysson, V. Fuchs, I. P. Shkarofsky, P. Bonoli

Décembre 1992

CEA EURATOM

ASSOCIATION EURATOM-C.E.A.
DEPARTEMENT DE RECHERCHES SUR LA FUSION CONTROLEE
C.E.N./CADARACHE
13108 SAINT-PAUL LEZ DURANCE CEDEX

ADJOINT OPTIMIZATION SCHEME FOR LOWER HYBRID CURRENT RAMPUP AND PROFILE CONTROL IN TOKAMAKS

X. Litaudon, D. Moreau, J. P. Bizarro, G. T. Hoang, K. Kupfer, Y. Peysson,
V. Fuchs[1], I. P. Shkarofsky[2], P. Bonoli[3]

Département de Recherches sur la Fusion Contrôlée,
Association Euratom-CEA
Centre d' Etudes de Cadarache,
13108 St. Paul lez Durance Cedex, France

[1] Centre Canadien de Fusion Magnétique, Hydro-Québec, Varennes, Québec, Canada
[2] MPB Technologies, Dorval, Québec, Canada
[3] Plasma Fusion Center, Massachusetts Institute of Technology,
Cambridge, MA 02173, USA

ABSTRACT

The purpose of this work is to take into account and study the effect of the electric field profiles on the Lower Hybrid (LH) current drive efficiency during transient phases such as rampup. As a complement to the full ray-tracing / Fokker Planck studies, and for the purpose of optimization studies, we developped a simplified 1-D model based on the adjoint Karney-Fisch numerical results. This approach allows us to estimate the LH power deposition profile which would be required for ramping the current with prescribed rate, total current density profile (q-profile) and surface loop voltage. For rampup optimization studies, we can therefore scan the whole parameter space and eliminate a posteriori those scenarios which correspond to unrealistic deposition profiles. We thus obtain the time evolution of the LH power, minor radius of the plasma, volt-second consumption and total energy dissipated. Optimization can thus be performed with respect to any of those criteria. This scheme is illustrated by some numerical simulations performed with TORE-SUPRA and NET/ITER parameters. We conclude with a derivation of a simple and general scaling law for the flux consumption during the rampup phase.

CONTENTS

1. INTRODUCTION

2. DESCRIPTION OF THE 1-D MODEL

3. APPLICATIONS TO TORE SUPRA AND NET/ITER

4. INTERPRETATION OF (P^*, $\Delta\Phi^*$) IN THE ZERO-D LIMIT

5. CONCLUSIONS

ACKNOWLEDGEMENTS

APPENDIX

REFERENCES

FIGURE CAPTIONS

1. INTRODUCTION

To complement the full ray-tracing/Fokker Planck studies[1-2], and for the purpose of rampup optimization studies, we developped a simple 1-D model based on the adjoint Karney-Fisch numerical results[3]. Rather than performing full simulations with tentative power spectra, the question which is raised here is the more general one : How can we vary the rf power waveform and deposition profile and possibly the minor radius of the plasma and, such that not only the edge safety factor, q_a, is constant, but also the radial q-profile is controlled during the rampup phase ?

In this approach, the total current density profile is prescribed as a function of time (q-profile), and the surface loop voltage (i.e. flux consumption) is given. It is then possible to determine the ohmic component of the current density profile and therefore the required rf driven current as a function of radius and time. Using the generalized Lower Hybrid (LH) current rampup efficiency computed numerically from the adjoint formalism, we can thus obtain the LH power waveform and deposition requirements consistent with the prescribed q-profile, rampup rate and flux consumption. In this study, a Poynting analysis[4] (based on the integral form of the Poynting theorem) is used for evaluating the flux consumption.

The problem is well-posed in the sense that, for a given scenario (q-profile, rampup rate and surface loop voltage), the solution for the rf power deposition at a given time is unique. Furthermore, since the proposed scheme does not use large code simulations, we can easily scan the whole parameter space (rampup rate, flux, ...) and eliminate a posteriori those scenarios which correspond to unrealistic deposition profiles. For the purpose of optimizing rf-assisted rampup scenarios, i.e. of defining "ideal" scenarios for a given set of constraints, the flux saving and stability problems are thus decoupled from the difficult, CPU-time consuming wave propagation problem[1-2]. Of course, ray-tracing studies can then be made separately for assessing which LH power spectra should be launched to obtain the desired "ideal" deposition profiles versus time, or a least to get as close as possible to them.

As outputs of the calculation, in addition to the required power deposition profiles, we also obtain the time evolution of the LH power, minor radius of the plasma, volt-second consumption, total launched rf energy and total energy dissipated. Optimization can thus be performed with respect to any criteria on those quantities.

We describe the 1-D rampup model in section 2. In section 3, we illustrate the method by some numerical results obtained with the TORE SUPRA and NET/ITER parameters. We conclude in section 4 with an interpretation of the numerical results and with a derivation of a simple and general scaling law for the flux consumption.

2. DESCRIPTION OF THE 1-D MODEL

Let us assume that the prescribed q-profile has the simple analytic form :

$$q(r,t) = q_o + (q_a - q_o)\left(\frac{r}{a(t)}\right)^{\gamma} \qquad (1)$$

where q_o and q_a (respectively the central and plasma edge safety factor) are constant during the current rise ; a(t) is the minor radius of the plasma column. Other analytic forms could be used but, in this report, we shall restrict ourselves to this monotonic function.

The purpose of this work is to take into account and study the effect of the electric field profile on the current drive efficiency during transient phases such as rampup. We shall therefore neglect phenomena such as plasma motion and constraints due to MHD equilibrium. The solution of the general time dependent plasma evolution and equilibrium is far beyond the scope of this work and is only tractable with a large scale numerical simulation[5-6]. We are indeed considering both the large aspect-ratio and low-beta limits (where beta is the ratio of the plasma pressure to the magnetic pressure), i.e. order zero of the Shafranov's aspect ratio expansion of the magnetic field. The plasma is supposed to be made of concentric circular flux surfaces on which the fluid is at rest at all times. The radius of the plasma column can be allowed to vary by ad hoc ionization of the external layers.

We use the appropriate cylindrical co-ordinate (r, θ, ϕ) where r is the radial position , θ the poloidal angle and ϕ the toroidal angle. In the cylindrical limit the q-profile is related to the vacuum equilibrium static toroidal field, B_o, and poloidal field, B_θ , according to the relation:

$$q(r,t) = \frac{r\, B_o}{R_o\, B_\theta\,(r,t)}$$

and

$$q_a = \frac{2\pi\, a^2(t)\;\; B_o}{\mu_o R_o\, I_p\,(t)}$$

where R_o is the major radius and $I_p(t)$ the plasma current. The edge safety factor is maintained constant during the current rise if the minor radius is varied at a rate :

$$\frac{\dot{a}(t)}{a(t)} = \frac{1}{2}\frac{\dot{I}_p(t)}{I_p} \qquad (2)$$

with

$$\dot{a}(t) = \frac{da(t)}{dt} \qquad \dot{I}_p(t) = \frac{dI_p(t)}{dt}$$

The toroidal current density, J_ϕ, and toroidal electric field, E_ϕ, corresponding to the prescribed q-profile are solutions of the Maxwell's equations written in the laboratory frame and using the appropriate cylindrical coordinates :

$$\frac{\partial E_\Phi(r,t)}{\partial r} = \frac{\partial B_\theta(r,t)}{\partial t} \tag{3-a}$$

$$\frac{1}{r}\frac{\partial r E_\theta(r,t)}{\partial r} = -\frac{\partial B_\phi(r,t)}{\partial t} \tag{3-b}$$

$$-\frac{\partial B_\phi(r,t)}{\partial r} = \mu_o j_\theta(r,t) \tag{4-a}$$

$$\frac{1}{r}\frac{\partial r B_\theta(r,t)}{\partial r} = \mu_o j_\phi(r,t) \tag{4-b}$$

where B_ϕ, j_θ, and E_θ are respectively the plasma toroidal magnetic field, the poloidal current and poloidal electric field. Assuming that the toroidal field is the vacuum field B_o, which has no radial and time dependence, one shows with equations (3-b) and (4-a) that the poloidal component of the electric field, E_θ, and the poloidal current, j_θ, vanish in the plasma column. For the following calculations, we are considering the equations (3-a) and (4-b).
The poloidal field is deduced from the q profile :

$$B_\theta(r,t) = \frac{r B_o}{R_o q(r,t)}$$

Consequently the total current density profile obtained from the Ampere's law is linked to the q-profile according to:

$$J_\Phi(r,t) = \frac{2 B_o}{\mu_o R_o q(r,t)}\left\{1 - \frac{1}{2} s(r,t)\right\} \tag{5}$$

where s(r,t) is the magnetic shear :

$$s(r,t) = \frac{r}{q(r,t)}\frac{\partial q(r,t)}{\partial r}$$

In order to set the current density profile at the limiter radius to zero, we choose the exponent γ in the q-profile as :

$$\gamma = \frac{2 q_a}{(q_a - q_o)}$$

The time evolution of the poloidal field is given by :

$$\frac{\partial B_\theta (r,t)}{\partial t} = - \frac{r\, B_o}{R_o\, q^2(r,t)} \frac{\partial q(r,t)}{\partial t}$$

Differentiating with respect to time the q-profile equation (1) leads to:

$$\frac{\partial q(r,t)}{\partial t} = - \gamma (q_a - q_o) \frac{\dot{a}(t)}{a(t)} \left(\frac{r}{a(t)}\right)^\gamma$$

The electric field profile is deduced from the time evolution of the poloidal magnetic field, i. e. Faraday's law (eq. 3-a). It is therefore solution of the first order differential equation :

$$\frac{\partial E_\Phi (r,t)}{\partial r} = \frac{a(t)\, \dot{I}_p(t)\, B_o\, \gamma (q_a - q_o)}{2\, I_p\, R_o\, q^2(r,t)} \left(\frac{r}{a(t)}\right)^{\gamma+1} \qquad (6)$$

The constant of integration is determined by using a voltage boundary condition at the plasma surface, $r = a(t)$:

$$E_\phi (a,t) = \frac{V_s}{2\pi R_o}$$

where the plasma surface loop voltage, V_S , is taken constant during the current rise.
We introduce the reduced variable, $x=r/a(t)$, which falls into the fixed interval [0,1]. Using this normalised radius we express the electric field profile in terms of the rampup rate, loop voltage, and a profile function F(x) :

$$E_\phi (x) = - \dot{I}_p F(x) + \frac{V_s}{2\pi R_o} \qquad (7)$$

where

$$F(x) = \frac{\mu_o q_a \gamma (q_a - q_o)}{4\pi} \int_x^1 \frac{x^{\gamma+1}}{q(x)^2}\, dx$$

The solution shows that during rampup with a prescribed q-profile, rampup rate and loop voltage, the electric field profile written in the normalised variable is frozen. Moreover, it shows the effect of varying the rampup rate and/or loop voltage on the electric field profile.

Once the electric field profile is known, we calculate the electron temperature profile and the rf power deposition profile self consistently through an iterative process, as shown below.

Starting from a first guess of the electron temperature profile, the ohm's law determines the ohmic current density profile (J_{oh}) :

$$J_{oh}(r,t) = \sigma(r,t)\, E_{\phi}(r,t) \tag{8}$$

where σ is the neoclassical conductivity[7].

The rf current density profile J_{rf} is obtained by substracting the ohmic current density profile to the total current density profile :

$$J_{rf}(r,t) = J_{\phi}(r,t) - J_{oh}(r,t) \tag{9}$$

The power, P_{el} , which results from the interaction of the rf-driven current with the inductive electric field is defined as in ref.3 :

$$P_{el}(r,t) = - J_{rf}(r,t)\, E_{\phi}(r,t) \tag{10}$$

When the electric field is negative, the suprathermal electrons are decelerated and the corresponding power, P_{el}, goes into the poloidal field energy. When the electric field is positive, both the rf power and the electric field accelerate the electrons in the same direction.

In writing the constitutive equations (8) and (10), we have implicitly assumed that the axial component of the electric field is roughly equal to its parallel component, i.e. parallel to the total magnetic field. Such an approximation is consistent with the large aspect-ratio and low-beta limits that we have considered. Since, the parallel component of the electric field is invariant, this assumption is also consistent with the fact that we neglect any perpendicular motion of the fluid plasma.

The absorbed power density, P_{rf}, that results from quasilinear electron Landau damping of the Lower Hybrid waves is determined by :

$$P_{rf}(r,t) = \frac{P_{el}(r,t)}{\eta(r,t)} \tag{11}$$

When $P_{el} > 0$, η is a generalized local efficiency for converting rf energy into poloidal magnetic energy, and is calculated in the presence of a decelerating electric field[3]. If $P_{el} < 0$, $-P_{el}$ is simply the power given to the suprathermal electrons by the accelerating electric field. η depends on the ratio of the phase velocity to the Dreicer velocity.

Some fraction of P_{rf} provides bulk heating from the collisional slowing down of the fast electrons on thermal plasma electrons :

$$P^{s}_{col}(r,t) = P_{rf}(r,t) - P_{el}(r,t) \tag{12}$$

The ohmic heating source is :

$$P^{b}_{col}(r,t) = J_{oh}(r,t)\ E_{\Phi}(r,t) \tag{13}$$

The sum of the electron energy sources which provide electron bulk heating is then :

$$P_{diss}(r,t) = P^{b}_{col}(r,t) + P^{s}_{coll}(r,t) \tag{14-a}$$

or

$$P_{diss}(r,t) = J_{\Phi}(r,t)\ E_{\Phi}(r,t) + P_{rf}(r,t) \tag{14-b}$$

In the second step of the iteration procedure, a simplified 1-D radial transport equation is solved in order to obtain a new electron temperature profile which is consistent with the heating source:

$$-\frac{1}{r}\frac{\partial}{\partial r}\left[r\, n_e(r)\ \chi_e(r)\frac{\partial Te(r,t)}{\partial r}\right] = P_{diss}(r,t) \tag{15}$$

where n_e is the electron density profile, χ_e the electron thermal diffusivity, and we assume that the convection/conduction losses dominate over the time derivative of the stored electron energy (other loss terms are neglected).

The electron thermal diffusivity is assumed to be given by the relation :

$$\chi_e(r) = \frac{M_e}{r\, n_e(r)}$$

where M_e is a constant determined by matching the total stored electron energy to the one predicted by the Rebut-Lallia scalling[8] :

$$W_e^{R\text{-}L} = 2.610^{-2}\, \bar{n}_e^{3/4} Z_{eff}^{1/4}\, B_o^{1/2}\, I_p^{1/2} (R_o ab)^{11/12} + 1.210^{-2}\, I_p\, (R_o ab)^{1/2}\, Z_{eff}^{-1/2} P_{diss} \tag{16}$$

where P_{diss} is here the volume integral of P_{diss} (r,t) given in eq.(14). Other scaling laws could be used instead of (16), such as the ITER scaling.

Iterations can then proceed between the electron temperature profile deduced from eq.15 and the rf power deposition profile deduced from eq.(9-10-11). This process is repeated until the electron temperature converges towards a self-consistent profile.

3. APPLICATIONS TO TORE SUPRA AND NET/ITER

In order to illustrate this method, we now present some numerical results obtained with TORE-SUPRA and NET/ITER parameters.

3.a. TORE SUPRA numerical results

Let us impose a plasma current varying from 0.8 MA to 1.6 MA with a monotonic q-profile (cf. eq.(1)), with q_o =1.0, q_a = 3.2 and a central density of 2.5 x 10^{19} m^{-3}. The minor radius must then be expanded from 0.55 m to the nominal value of 0.78 m. The electron density profile is chosen parabolic to the power 0.6. The major radius is R_0 = 2.34 m, the toroidal magnetic field is B_0 = 3.85 T and the rf power is supposed to be absorbed at an average parallel index $\langle n_{//} \rangle$ = 2.4, allowing for a small upshift in the course of propagation.

As an example, we first discuss the results for the case where the current is ramped at a rate dI_p/dt = 0.4 MA/s with a surface loop voltage of 0.55 Volts. We find that the LH power must be gradually increased from 2 MW to 4 MW at rate of 1MW/s (fig. 1 (a-b)). The total dissipated energy (W_{diss}) which is the time integral of the dissipated power (P_{diss}) during the current ramp reaches the value of 6.1 MJ. As a consequence of the electric field diffusion, the central ohmic density current is small (fig. 2-a). Thus an appreciable amount of rf current density must be generated at the plasma center (fig. 2-b) to maintain the desired total current density and internal plasma inductance to its fixed value of 1.28. The corresponding deposition profiles are given in fig.3 at different times during the current ramp.

For optimization purposes, we scan a large range of rampup rates and loop voltages. The rampup rate is varied from 0.025 to 1.025 MA/s by steps of 0.1MA/s, and for each rampup rate the surface loop voltage is taken successively as : - 0.2, - 0.15, - 0.1, - 0.05, 0, 0.05, 0.1, 0.15, 0.2, 0.5, 0.75, 1, 1.25 and 1.5 Volt. The maximum power required to ramp the plasma current at its final value of 1.6 MA, and the total dissipated energy (W_{diss}) are plotted versus the necessary flux in figs. 4 (a-b) and 5 (a-b) for various loop voltages or rampup rates. The curves have been truncated by the requirement that the power deposition profiles are reasonable (i. e. no reverse driven current is necessary). The maximum absorbed power diagrams, fig. 4 (a-b), exhibit two distinct regions separated by critical values of flux ($\Delta\Phi^*$) and LH power (P^*) at which all curves cross. These two regions are :

i) $\Phi > \Delta\Phi^*$ and $P < P^*$,

ii) $\Phi < \Delta\Phi^*$ and $P > P^*$.

For the TORE SUPRA parameters and the current rampup conditions which have been chosen, the values of $\Delta\Phi^*$ and P^* are respectively 0.9 Wb and 5 MW.

We now comment the numerical results obtained in the two regimes :

i) $\Phi > \Delta\Phi^*$ and $P < P^*$. At a fixed flux consumption, we find that the necessary rf power is lowest when the plasma current is ramped at the highest rate and surface loop voltage which are compatible with realistic deposition profiles. For instance, for a flux consumption of 1.6 Wb, it is shown on figure 4 (a-b) that the mimimum value of rf power (1 MW) is obtained with a rampup rate of 0.625 MA/s and a surface loop voltage of 1.25 Volt. Figure 5 (a-b) illustrates that such a current rampup scenario (high loop voltage and short rampup time compatible with the power profile requirements) also minimises the total dissipated energy.

ii) $\Phi < \Delta\Phi^*$ and $P > P^*$. At a fixed rf power, a large amount of flux is saved when the current is ramped slowly (low rampup rate) with a small loop voltage. With 5 MW of rf power, all the flux could be saved (the loop voltage is set to zero) by rising the current at a rate of 0.025 MA/s. The rampup phase would then last 32 seconds and the total dissipated energy would reach 116 MJ. Large flux savings are obtained at the expense of a long rampup time and therefore a large amount of total dissipated energy as shown in figure 5.

With the LH power which is available on TORE SUPRA (i.e., up to the 6 MW has been coupled during the 1.6 MA plasma current plateau), various current rampup scenarios can be tested. On the one hand, we have shown that a fast current rise where a high plasma surface loop voltage is applied, minimises the necessary rf power and total dissipated energy. On the other hand, we focus our attention on a low (or zero) flux consumption scenario, where the plasma current is ramped slowly together with a low (even zero) applied loop voltage. One can access this low flux consumption scenario only when either the corresponding dissipated energy stays within the load range of the limiter and/or inner wall, or when the dissipated power is continuously evacuated through an active cooling system.

A set of experiments will be carried out in order to study the experimental relevance of the two rampup regimes (i) $\Phi > \Delta\Phi^*$ and $P < P^*$; ii) $\Phi < \Delta\Phi^*$ and $P > P^*$) and possibly to investigate the low flux consumption scenario (ii).

3.b. NET / ITER numerical results

Let us first impose that the plasma current varies from 3.5 MA to 22 MA with a constant rate, a monotonic q-profile (cf. eq.1), with q_o =1.0, q_a = 2.2, and at a central density of 4 x 10^{19} m^{-3}. The corresponding plasma internal inductance is l_i = 1.06 and the electron density profile is chosen parabolic to the power 0.5. The minor radius must be expanded from 1.4 m to the nominal value of 3.4 m. The major radius is R_0 = 6.0 m, the toroidal magnetic field is B_0 = 4.85 T and the rf power is supposed to be absorbed at an average parallel index $<n_{//}>$ = 1.7.

It is then found that the incremental confinement time has to be degraded on purpose to prevent the electron temperature - and therefore the ohmic current density - to rise to unacceptable values. This is done by including a correction factor in the second term of equation (16). For simplicity we have assumed in this study that the incremental confinement time is zero, but this assumption could probably be relaxed to some extent.

If we select a rampup rate of 0.35 MA/s, and a surface loop voltage of 1 Volt, then the minor radius and the rf power must evolve in time as shown on fig.6 (a-b). We find that the LH power must be gradually increased from 15 MW to 70 MW at a rate of approximately 1 MW/s during the 53 second current rampup period. The corresponding deposition profiles are given in fig.7 at different times during the current rise.

The maximum power and total dissipated energy are plotted versus the necesssary flux consumption in fig. 8 (a-b).The results are obtained by scanning the rampup rates between 0.005 and 0.5 MA/s by steps of 0.05 MA/s, and for each rampup rate the loop voltage is successively taken as : 0.25, 0.5, 0.75, 1 and 1.5 Volt. As before, the curves are limited by the requirement that the power deposition profiles be reasonable, namely that no reverse driven current is necessary.

To reach a flattop 22 MA plasma current with a frozen q-profile, the previously defined critical values of flux consumption, $\Delta\Phi^*$, and rf power, P^*, are respectively 40 Wb and 140 MW. Thus with a maximum available LH power of 50 MW, the appropriate rampup regime to the nominal value of 22 MA must be the one identified previously, where $\Phi > \Delta\Phi^*$ and $P < P^*$ (cf. 3.a), except perhaps in the initial low current phase. In this regime figure 8 (a-b) shows that the minimum amount of LH power (36 MW) and total dissipated energy (1100 MJ) are obtained at a rampup rate of 0.5 MA/s and at a fixed loop voltage of 1.5 V. In those optimum conditions 870 MJ of lower hybrid slow wave energy is delivered gradually and the necessary flux consumption is 55 Wb.

In order to further reduce the flux consumption, it could be beneficial to drive the early stage of the current ramp in the low flux consumption regime ($\Phi < \Delta\Phi^*$ and $P > P^*$; cf. **3.a**). We find numerically that, up to a plasma current of 6 MA, the maximum available rf power (50 MW) is always above the critical value of P* which separates the two rampup regimes. Fig. 9 shows the dependence of P* with the plasma current, and numerically proves that P* = 37 MW when the plasma current rises to the intermediate value of 6 MA .

As an example of our optimisation scheme, we have studied more precisely the first stage of the current rise, where the plasma current is ramped between 3.5 MA and 6 MA, with the other NET parameters as before. To reach this intermediate value of plasma current (I_p = 6 MA), the necessary rf power and total dissipated energy have been calculated and plotted versus flux consumption in figures 10 (a-b) and 11 (a-b) for loop voltages of - 0.01, 0, 0.01, 0.05, 0.075, 0.1, 0.15, 0.25, 0.5, 0.75, 1 and 1.5 Volt, and rampup rates between 0.005 and 0.5 MA/s by steps of 0.05 MA/s. With 50 MW of rf power in this intermediate phase, one can in principle save all the flux (the loop voltage is set to zero) by slowly ramping the plasma current at a rate of 0.10 MA/s up to a plasma current of 6 MA. In this first stage of the current rise, the total dissipated energy would then reach 930 MJ. At a faster rate of 0.5 MA/s, only 400 MJ would be dissipated but the rf power would then have to be increased up to more than 100 MW.

In the second stage of the current rampup, i.e. from 6 MA to 22 MA where the low flux consumption regime is not accessible with 50 MW, increasing the rampup rate and loop voltage would minimise the rampup time and therefore the total dissipated energy. It must be noted that this second stage could possibly take place in the X-point divertor phase with active cooling of the divertor plates with power limitations but possibly no energy limitation.

4. INTERPRETATION OF (P*, ΔΦ*) IN THE ZERO-D LIMIT

Having, in the preceeding sections, studied quantitatively the influence of the profile effects during current rampup, we shall now give a simple interpretation of the results in terms of a zero-dimensional limit. We pointed out, in particular, the existence of a characteristic point in the (P, Φ) plane at which all curves approximately cross. The physical interpretation of this will be given here, as well as the scaling of the characteristic curves parametrized by the rampup rate with respect to dimensionless parameters.

In order to do so, and especially to characterize the two rampup regimes discussed above (cf. **3.a**), we define an effective loop voltage, $V_{eff}(t)$, as :

$$V_{eff} = 4\,\pi^2\, R_o \frac{a(t)^2}{I_p} \int_0^1 J_\phi(x)\; E_\phi(x)\; x dx \qquad (17)$$

which corresponds to a weighted average of the electric field through the plasma column, and which we can think of as the effective loop voltage in a zero-dimensional model of the plasma.

The plasma current can be written as the sum of the rf driven current and of an ohmic contribution. Neglecting the cross effect of the ohmic electric field and of the rf power, or equivalently the change in the plasma conductivity due to the suprathermal electrons, we simply write :

$$I_p = \eta\, P_{rf} + \frac{V_{eff}}{R_{sp}} = \eta\, P^* \qquad (18)$$

where η is the current drive efficiency (A/W), R_{sp} the Spitzer resistivity, and P* the rf power necessary to drive the full current I_p in steady-state.

The difference between the effective loop voltage and the surface loop voltage, V_{surf}, can be written in terms of the plasma current rampup rate. Using an effective inductance, L_{eff}, for the poloidal flux embraced between the plasma surface and the radius in the plasma at which $V = V_{eff}$, one writes :

$$V_{surf} = V_{eff} + L_{eff}\, \dot{I}_p \qquad (19)$$

where $L_{eff} = \frac{1}{2}\mu_o R_o (l_i - 0.5)$ and is constant (cf appendix),

or, in terms of fluxes, and with the convention that the flux consumptions, $\Delta\Phi_{surf}$, are counted positively whenever V_{surf} is positive :

$$\Delta\Phi_{surf} = V_{eff}\,\Delta t + L_{eff}\,\Delta I_p \tag{20}$$

Note that the flux consumption is defined as the time integral of V_{surf}. Because of the variation of the plasma surface, this is not to be confused with the difference between the initial and final fluxes at the plasma surface.

It is now straightforward to eliminate V_{eff} and $\Delta t = \Delta I_p/\dot{I}_p$ and to find the following linear approximation for the characteristic curves, around the point $(P^*, \Delta\Phi^*)$:

$$\left(\frac{P_{rf}}{P^*} - 1\right) = -\frac{\Delta\Phi^*}{\Delta\Phi_{sp}}\left(\frac{\Delta\Phi_{surf}}{\Delta\Phi^*} - 1\right) \tag{21}$$

where $\Delta\Phi^* = L_{eff}\,\Delta I_p$ and $\Delta\Phi_{sp} = R_{sp}\,I_p\,\Delta t$. Note that the critical flux $\Delta\Phi_{surf} = \Delta\Phi^*$ corresponds to $V_{eff} = 0$, i.e. to a cancellation between the internal flux increase due to the current ramp, and the external flux decrease inducing the surface voltage, as sketched on figure 12. Using a Poynting analysis (cf appendix), Ejima[4] et al. have identified the flux term, $\Delta\Phi^*$, as the inductive flux which is required to establish the magnetic configuration.

We can rewrite the slope of the curves in terms of two characteristic times, the resistive time, $\tau_{res} = L_{eff}/R_{sp}$, and the rampup time, $\tau_{Ip} = I_p/\dot{I}_p$, so that our characteristic equation (21) reads :

$$\left(\frac{\Delta\Phi_{surf}}{\Delta\Phi^*} - 1\right) = -\frac{\tau_{Ip}}{\tau_{res}}\left(\frac{P_{rf}}{P^*} - 1\right) \tag{22}$$

If ones takes the critical flux, $\Delta\Phi^*$, as a reference for the flux consumption corresponding to a given current increment, ΔI_p, the flux saving can be defined as :

$$\Phi_{saved} = \Delta\Phi^* - \Delta\Phi_{surf} \tag{23}$$

with the convention that the saving is negative when $\Delta\Phi_{surf} > \Delta\Phi^*$. Thus we have :

$$\frac{\Phi_{saved}}{\Delta\Phi^*} = \frac{\tau_{Ip}}{\tau_{res}}\left(\frac{P_{rf}}{P^*} - 1\right) \tag{24}$$

From this equation, the two regimes discussed previously are easily recognized :

i) when $P_{rf} < P^*$, the flux saving is negative (with our convention) and therefore, for a given ratio P_{rf}/P^*, one should minimize the ratio τ_{Ip}/τ_{res}. This can be done by

ramping the current as fast as possible, i.e. with a characteristic time scale which is small with respect to the ohmic current diffusion time, and also by maintaining τ_{res} as large as possible (high electron temperature, small Z_{eff}). This is a regime in which both the rf and ohmic currents add up, with the ohmic current localized in the outer parts of the plasma and the rf current filling up the center so as to maintain a stable q-profile.

ii) on the contrary, when $P > P^*$, which is in general possible in the low current initial phase, τ_{Ip}/τ_{res} should be maximized. The rampup rate should be minimum for large flux savings - namely much smaller than the inverse resistive diffusion time - and the plasma should be maintained as resistive as possible (low electron temperature, high Z_{eff}) because the effective electric field in the plasma is negative, driving an opposing ohmic current. For a given surface voltage, a small rampup rate prevents this field to become too much negative in the center of the discharge, which would in turn require too large LH powers.

5. CONCLUSIONS

In this work we have developped a 1-D model based on the adjoint Karney-Fisch numerical results[3] in order to take into account and study the effect of the electric field profile on the LH current drive efficiency during the LH assisted rampup phases. In this approach the q-profile is prescribed as function of time, and we deduce the required rf power waveform and deposition profiles. In order to maintain a monotonic q-profile during the rampup phase, we find that we need to increase the RF power gradually during the same time interval as the plasma current.

Since the proposed scheme does not use large code simulations, we have easily scanned the whole parameter space (rampup rate, flux consumption,...). Therefore an optimization study has been performed with the TORE SUPRA and NET/ITER parameters. Such study has clearly illustrated two rampup regimes where the RF power is either above ("overdriven" regime) or below ("underdriven" regime) the power required to steadily drives the full current.

Moreover, a general flux consumption scaling has been found from 0-D considerations and has been confirmed by the 1-D numerical calculations. Such flux consumption scaling shows that the flux economy is optimized in the "overdriven regime" when the ratio of the rampup time to the resistive time is maximized (low rampup rate, low plasma conductivity). In the "underdriven regime" the ratio of the rampup time to the resistive time should be minimized (high rampup rate, high plasma conductivity) to minimize the flux consumption.

To conclude, we stress that this study is a starting point for a more complete work using evolutive or semi-evolutive codes. In such codes, for instance SKENE [6], the flux consumption is consistently related to the plasma evolution and to the technological constraints on the poloidal field system.

ACKNOWLEDGEMENTS

This report is part of a Joint Final Report on contract NET/90-251. The authors whish to thank Dr. J. G. Wégrowe for its interest in this work.

APPENDIX

A.1 Determination of the effective inductance (L_{eff})

The flux of the Poynting's vector ($V_s\ I_p$) throught the boundary surface of the plasma volume, at a given time during the current ramp:

$$V_s\ I_p = \frac{\partial W_i}{\partial t} + V_{eff}\ I_p \qquad \text{(A1)}$$

where V_{eff} has been defined by the equation (17) and where the time derivative of the magnetic energy is :

$$\frac{\partial W_i}{\partial t} = 4\pi^2\ R_O \int_0^{a(t)} \frac{\partial}{\partial t} \frac{B_\theta^2(r,t)}{2\,\mu_0}\ r\ dr \qquad \text{(A2)}$$

or

$$\frac{\partial W_i}{\partial t} = \frac{4\pi^2\ R_O}{\mu_0} \int_0^{a(t)} B_\theta(r,t)\ \frac{\partial B_\theta(r,t)}{\partial t}\ r\ dr$$

We insert in equation (A2) the time evolution of the poloidal field, given by equation (3) and (6), in order to express the rate of change of the magnetic energy as :

$$\frac{\partial W_i}{\partial t} = L_{eff}\ I_p \dot{I}_p \qquad \text{(A3)}$$

where

$$L_{eff} = \frac{1}{2}\ \mu_o\ R_o\ l_{eff}$$

and

$$l_{eff} = q_a^2\ \gamma\ (q_a - q_o) \int_0^1 \frac{x^{\gamma+3}}{q^3(x)}\ dx$$

Note that l_{eff} is constant during the current rise

Using these notations the Poynting's theorem can be casted into the following form:

$$V_s\ I_p = L_{eff}\ I_p \dot{I}_p + V_{eff}\ I_p \qquad \text{(A4)}$$

Dividing by Ip equation (A4), we obtain the relation (19).

A.2 Determination of the internal inductance

The internal magnetic inductance (l_i) is definined as the average over the plasma volume (V) of the magnetic energy density :

$$l_i = \frac{\int_V \frac{B_\theta^2(r,t)}{2\mu_o} dV}{\frac{B_\theta^2(a,t)}{2\mu_o} V} \qquad (A5)$$

Using the Ampère's law, we write relation (A4) as :

$$l_i = \frac{4\ W_i}{\mu_o R_o\ I_p} \qquad (A6)$$

where W_i the magnetic energy :

$$W_i = 4\pi^2 R_o \int_0^{a(t)} \frac{B_\theta^2(r,t)}{2\mu_o} rdr$$

In order to express l_i in term of the q-profile, we insert in (A5) the poloidal field expression :

$$l_i = 2 q_a^2 \int_o^1 \frac{x^3}{q^2(x)} dx \qquad (A7)$$

Note that l_i is a constant during the current rise.

A.3 Relation between the effective inductance and the internal inductance

The stored magnetic energy is:

$$W_i = \frac{1}{2} L_i I_p^2 \qquad \text{with} \qquad L_i = \frac{1}{2} \mu_o R_o l_i \tag{A8}$$

Since, we have have shown that the internal inductance is constant, the total time derivative of the magnetic energy is simply :

$$\frac{dW_i}{dt} = L_i I_p \dot{I}_p \tag{A9}$$

To derive the relation between L_i and L_{eff}, one has to find a relation between the total time derivative and the partial time derivative of the magnetic energy. If one derives equation (A6), we obtain :

$$\frac{dW_i}{dt} = \frac{\partial W_i}{\partial t} + 4\pi^2 R_o \dot{a}\, a \frac{B_\theta^2(a,t)}{2\mu_o} \tag{A10}$$

Using the ampère's law, we express the poloidal field in terms of plasma current and using relation (2), we write the (A10) as:

$$L_i I_p \dot{I}_p = L_{eff} I_p \dot{I}_p + \frac{1}{4} R_o \mu_o I_p \dot{I}_p \tag{A11}$$

Consequently the normalised effective inductance (l_{eff}) and the normalised internal inductance (l_i) are linked by the simple relation :

$$l_{eff} = l_i - \frac{1}{2} \tag{A12}$$

REFERENCES

[1] V. Fuchs, I.P. Shkarofsky, P. Bonoli, J. P. Bizarro, X. Litaudon, D. Moreau, G.T. Hoang, K. Kupfer, Y. Peysson, Studies of lower-hybrid-assisted current rampup in the NET device, Rep. CCFM RI 381e, Centre canadien de fusion magnétique (1992).

[2] J. P. Bizarro, D. Moreau, On ray stochasticity during lower hybrid current drive in tokamaks, Rep. EUR-CEA-FC-1467, Centre d'études de Cadarache (1992) .

[3] C.F.F. Karney, N.J. Fisch, Phys. Fluids , **29**, (1986) 100.

[4] S.Ejima, R. W. Callis, J.L. Luxon, R.D. Stambaugh, T.S., Taylor, J.C. Wesley, Nuc. Fus., **22**, (1982) 1313.

[5] J. Blum, B. Saramito, Equilibrium - Transport and Stability of a plasma in a tokamak, Rep. EUR-CEA-FC-1375, Centre d'études de Cadarache (1989).

[6] J. M. Ané, J.P. Allibert, P. Hertout, in private communication.

[7] S. P. Hirshman, Phys. Fluids, **31**, (1988) 3150.

[8] P. H. Rebut, P. P. Lallia, M. L. Watkins, in Plasma Physics and controlled Nuclear Fusion Research, Proceedings of 12th International Conference, Nice, 1988 (IAEA,Vienna,1989), Vol. 2, P. 191.

FIGURE CAPTIONS

Fig. 1 TORE SUPRA : The plasma current is ramped from 0.8 to 1.6 MA at a rate of 0.4 MA/s. V_S = 0.55 V, q_o =1.0, q_a=3.2, R_o = 2.34 m, B_o=3.85 T, $\langle n_{//} \rangle$ = 2.4, n_{eo} = 2.5 x 10^{19} m^{-3} ;

(a) Minor radius versus time,

(b) LH power versus time.

Fig. 2 (a) Ohmic current density profiles,

(b) rf current density profiles.

The TORE SUPRA parameters and the rampup conditions are the same as in figure 1.

Fig. 3 Power density profile.

The TORE SUPRA parameters and the rampup conditions are the same as in figure 1.

Fig. 4 (a) Maximum absorbed power versus flux consumption for various loop voltages and rampup rates. The rampup rate is varied from 0.025 to 1.025 MA/s by steps of 0.1MA/s, and for each rampup rate the surface loop voltage is taken successively as : - 0.2, - 0.15, - 0.1, - 0.05, 0, 0.05, 0.1, 0.15, 0.2, 0.5, 0.75, 1, 1.25 and 1.5 Volt.

(b) Maximum absorbed power vs flux consumption for the same parameters as in (a).

The other TORE SUPRA parameters are the same as in figure 1.

Fig. 5 (a) Total dissipated energy versus flux consumption for various surface loop voltages ranging from - 0.2 to 1.5 Volt (as in fig. 4),

(b) Total dissipated energy versus flux consumption for various rampup rates ranging from 0.025 MA/s to 1.025 MA/s (as in fig. 4).

The other TORE SUPRA parameters are the same as in figure 1.

Fig. 6 NET/ITER : The plasma current is ramped from 3.5 to 22 MA at a rate of 0.35 MA/s. V_S = 1 V, q_o =1.0, q_a=2.2, R_o = 6.0 m, B_o= 4.85 T, $\langle n_{//} \rangle$ = 1.7, n_{eo} = 4.0 x 10^{19} m^{-3} ;

(a) Minor radius versus time,

(b) LH power versus time.

Fig. 7 Power density profile.

The NET parameters and the rampup conditions are the same as in figure 6.

Fig. 8 (a) Maximum absorbed power versus flux consumption for various loop voltages and rampup rates. The rampup rate is varied from 0.005 to 0.5 MA/s by steps of 0.05 MA/s, and for each rampup rate the loop voltage is successively taken as : 0.25, 0.5, 0.75, 1 and 1.5 Volt.

(b) Total dissipated energy versus flux consumption for the same parameters as in (a). Other parameters are the same as in figure 6.

Fig. 9 (a) Critical values of P* versus final plasma current ;

(b) Critical value of $\Delta\Phi^*$ versus plasma current increment.

The NET parameters are the same as in figure 6.

Fig. 10 NET/ITER : The plasma current is ramped from 3.5 to 6 MA. The other NET parameters are the same as in figure 6 ;

(a) Maximum absorbed power versus flux consumption for various loop voltages and rampup rates. The rampup rate is varied from 0.005 to 0.5 MA/s by steps of 0.05 MA/s, and for each rampup rate the loop voltage is successively taken as : - 0.01, 0, 0.01, 0.05, 0.075, 0.1, 0.15, 0.25, 0.5, 0.75, 1 and 1.5 Volt.

(b) Maximum absorbed power vs flux consumption for the same parameters as in (a).

Fig. 11 (a) Total dissipated energy versus flux consumption for various loop voltages ranging from - 0.01to 1.5 Volt (as in fig.10).

(b) Total dissipated energy versus flux consumption for various rampup rates ranging from 0.005 MA/s to 0.5 MA/s (as in fig.10).

The other NET parameters and rampup conditions are the same as in figure 6.

Fig. 12 Schematic representation of the cancellation between the internal and external poloidal flux (in the zero-dimensional limit) corresponding to the critical flux : $\Delta\Phi_{surf} = \Delta\Phi^*$ ($V_{eff} = 0$). Poloidal cross-section of the plasma column.

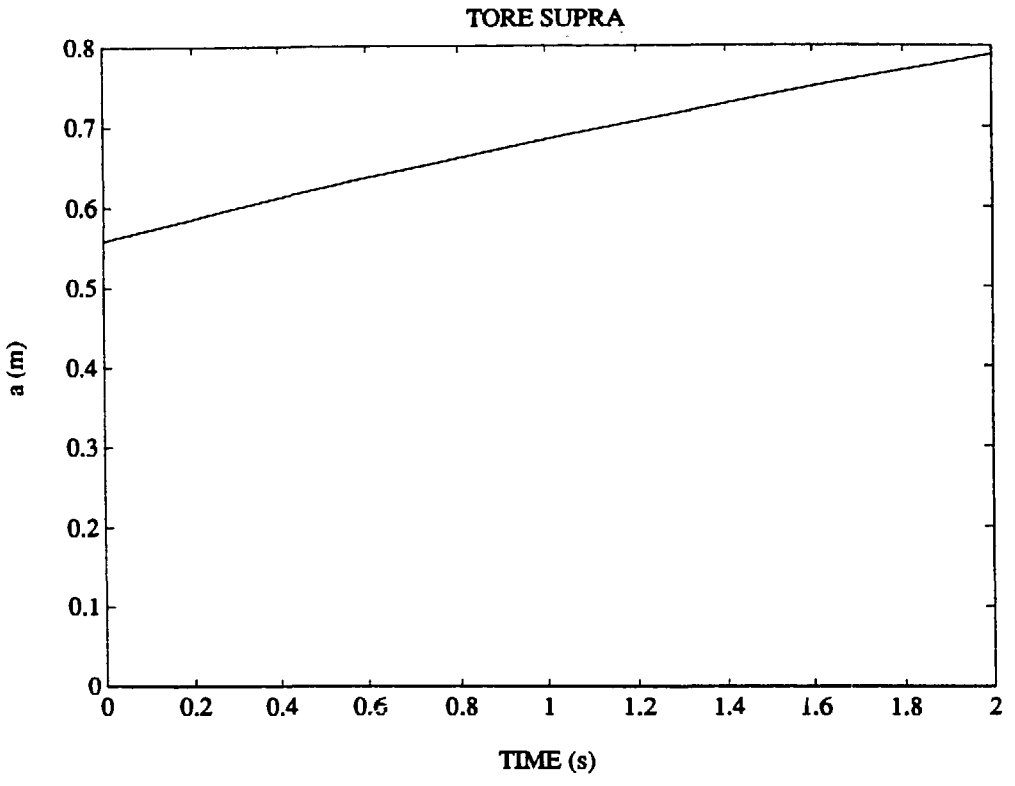
TORE SUPRA
a (m)
0.8
0.7
0.6
0.5
0.4
0.3
0.2
0.1
0
0
0.2
0.4
0.6
0.8
1
1.2
1.4
1.6
1.8
2
TIME (s)

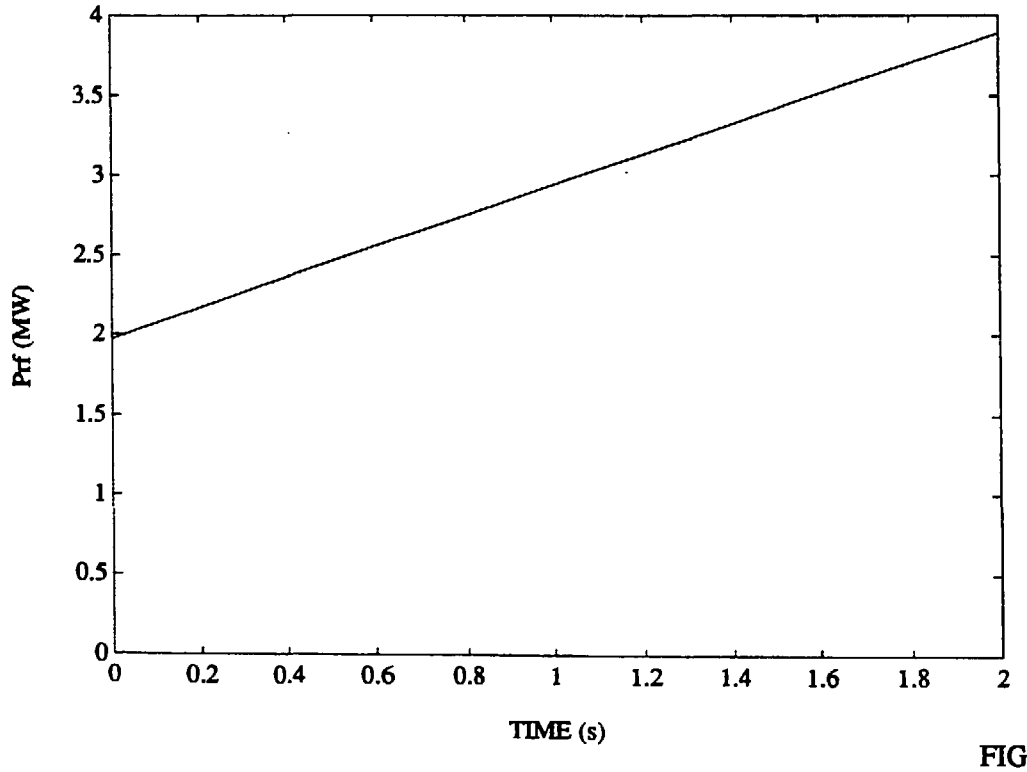
Prf (MW)
4
3.5
3
2.5
2
1.5
1
0.5
0
0
0.2
0.4
0.6
0.8
1
1.2
1.4
1.6
1.8
2
TIME (s)

FIGURE 1

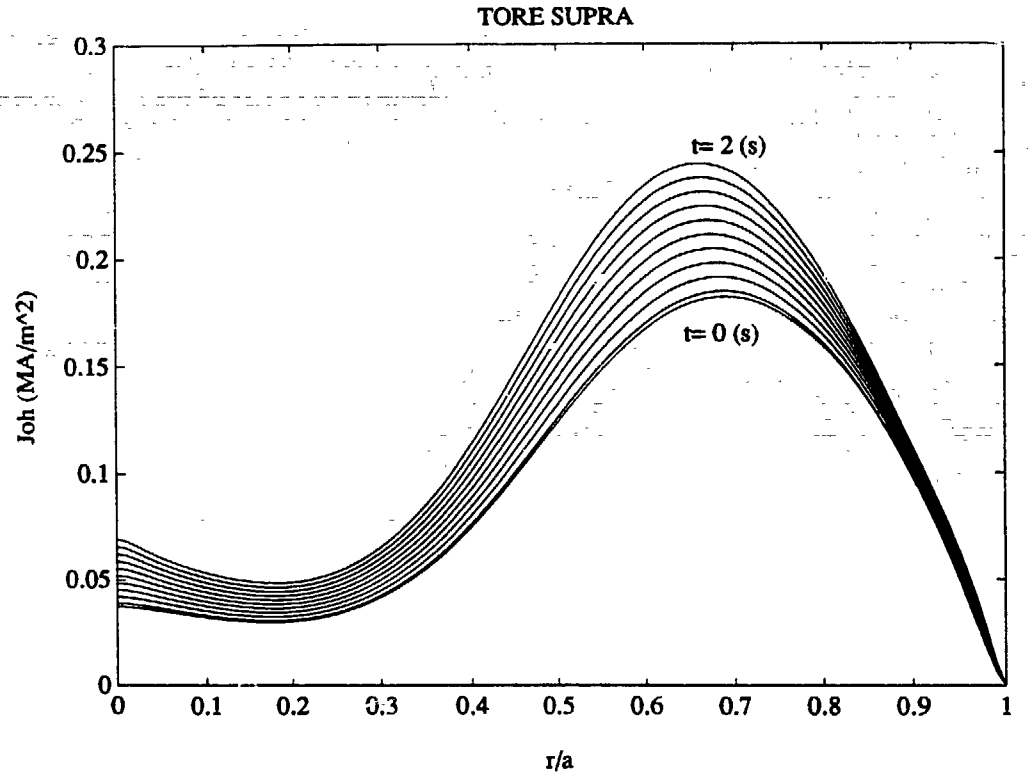
TORE SUPRA
t= 2 (s)
t= 0 (s)
Joh (MA/m^2)
r/a
0
0.05
0.1
0.15
0.2
0.25
0.3
0.1
0.2
0.3
0.4
0.5
0.6
0.7
0.8
0.9
1

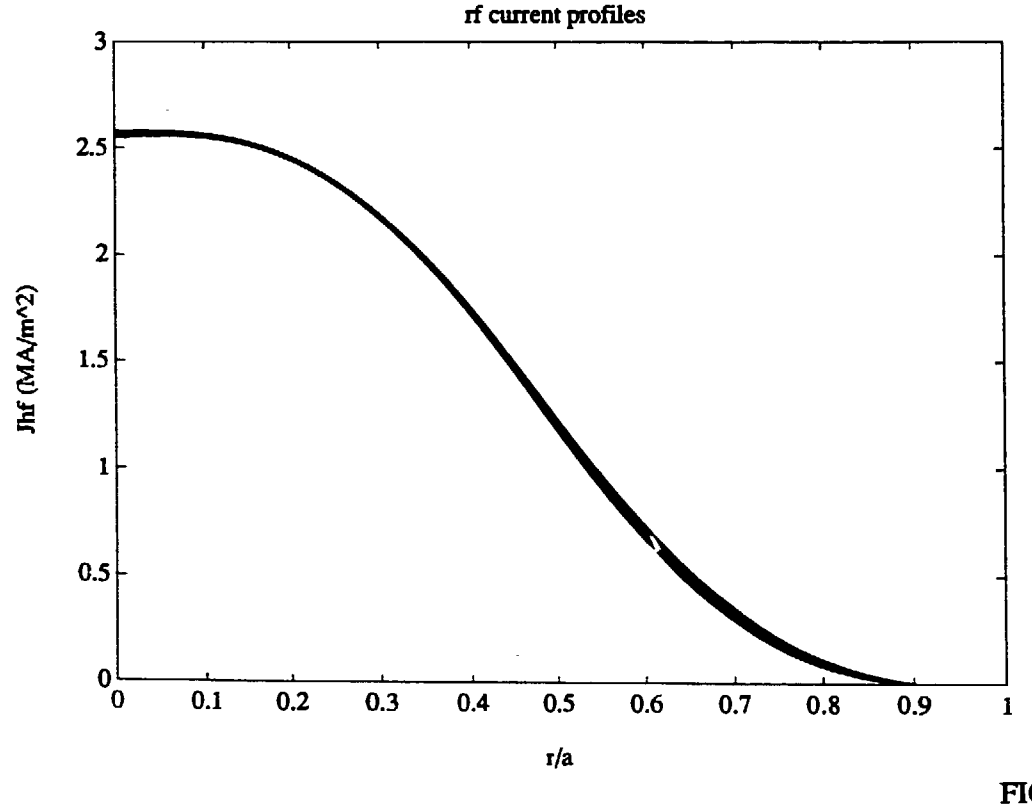
rf current profiles
Jhf (MA/m^2)
r/a
0
0.5
1
1.5
2
2.5
3
0.1
0.2
0.3
0.4
0.5
0.6
0.7
0.8
0.9
1

FIGURE 2

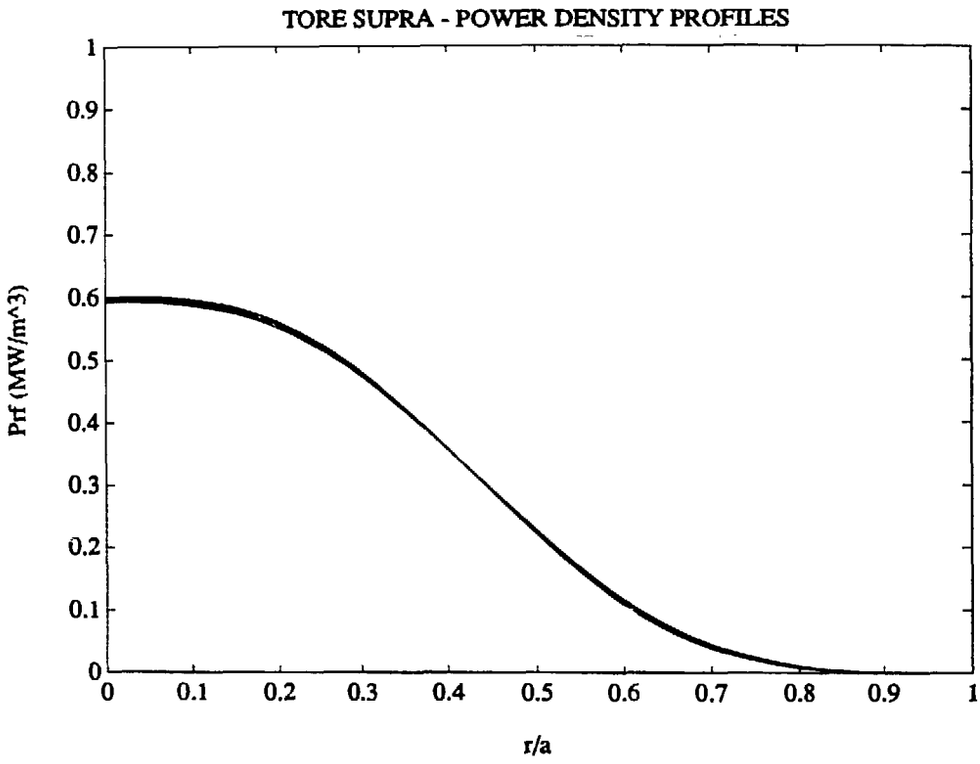
TORE SUPRA - POWER DENSITY PROFILES
Prf (MW/m^3)
r/a
0
0.1
0.2
0.3
0.4
0.5
0.6
0.7
0.8
0.9
1

FIGURE 3

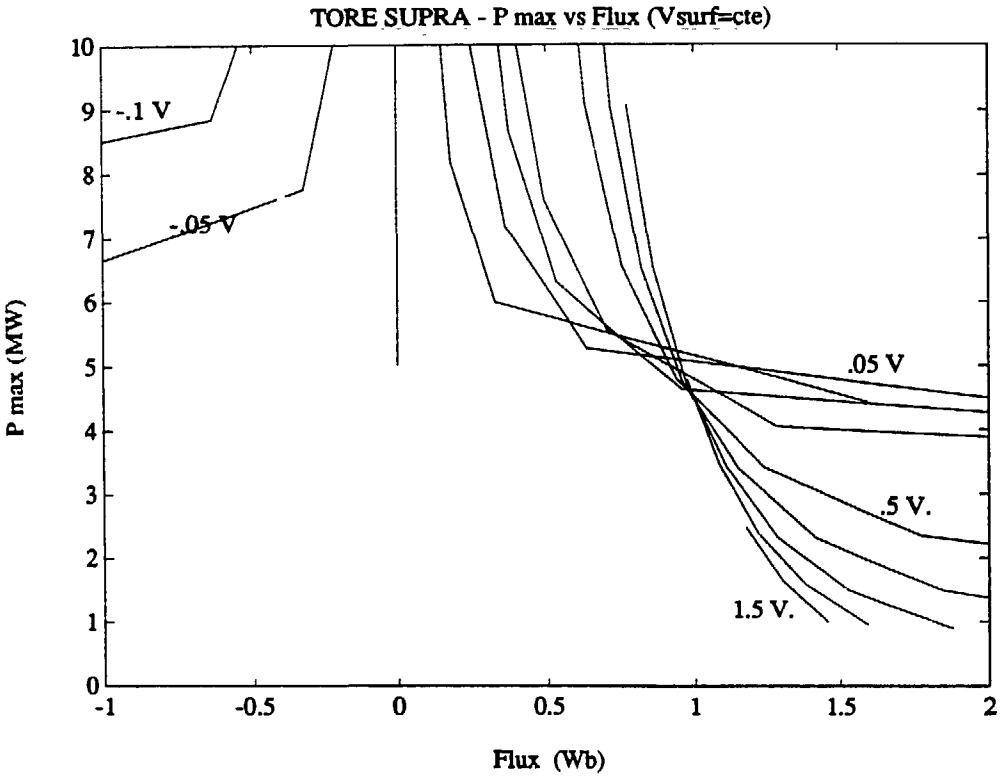
TORE SUPRA - P max vs Flux (Vsurf=cte)
P max (MW)
Flux (Wb)
-.1 V
-.05 V
.05 V
.5 V.
1.5 V.
10
9
8
7
6
5
4
3
2
1
0
-1
-0.5
0
0.5
1
1.5
2

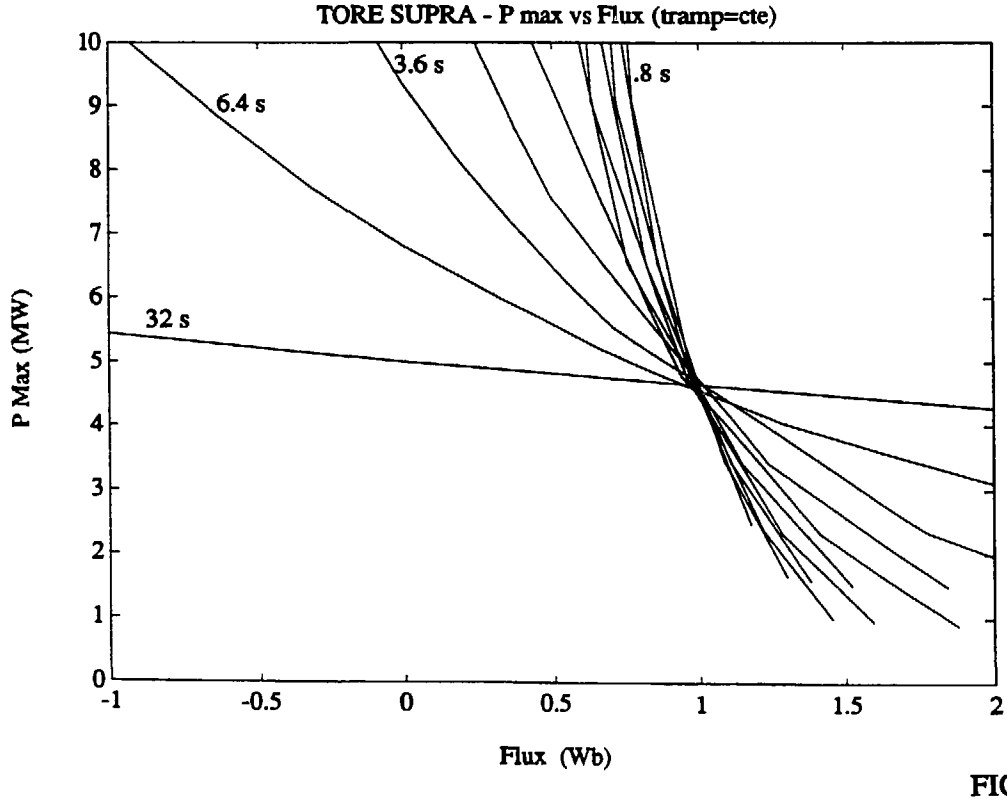
TORE SUPRA - P max vs Flux (tramp=cte)
P Max (MW)
Flux (Wb)
3.6 s
.8 s
6.4 s
32 s
10
9
8
7
6
5
4
3
2
1
0
-1
-0.5
0
0.5
1
1.5
2

FIGURE 4

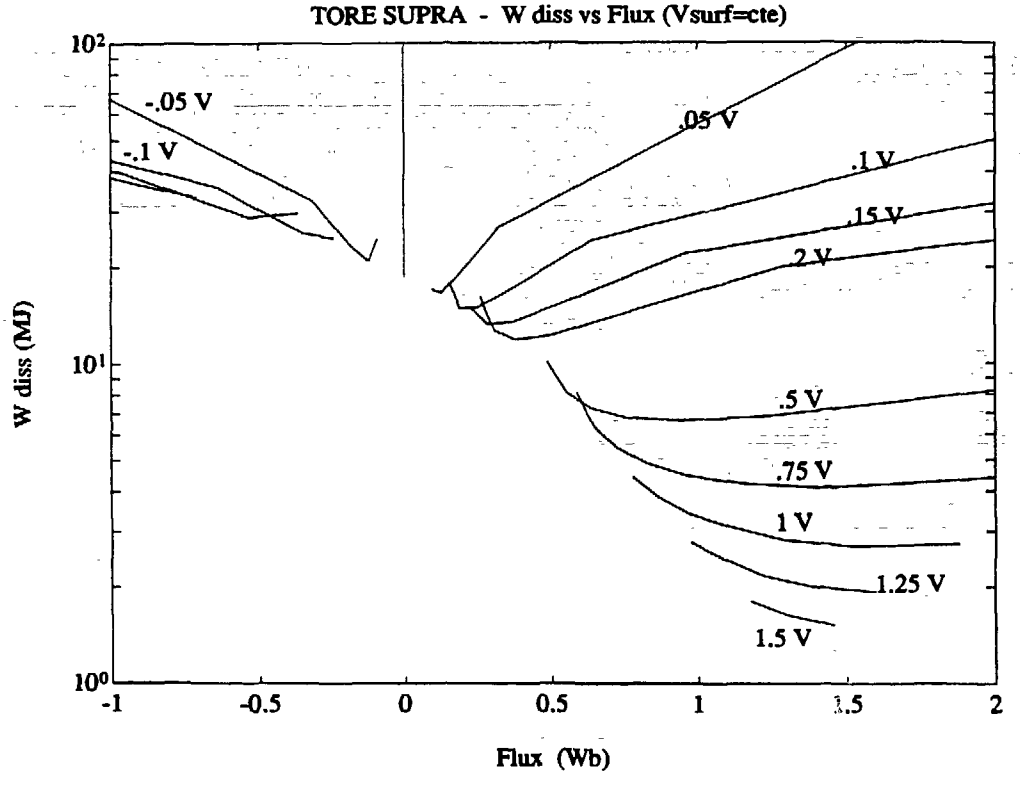
TORE SUPRA - W diss vs Flux (Vsurf=cte)
W diss (MJ)
Flux (Wb)
-.05 V
-.1 V
.05 V
.1 V
.15 V
.2 V
.5 V
.75 V
1 V
1.25 V
1.5 V

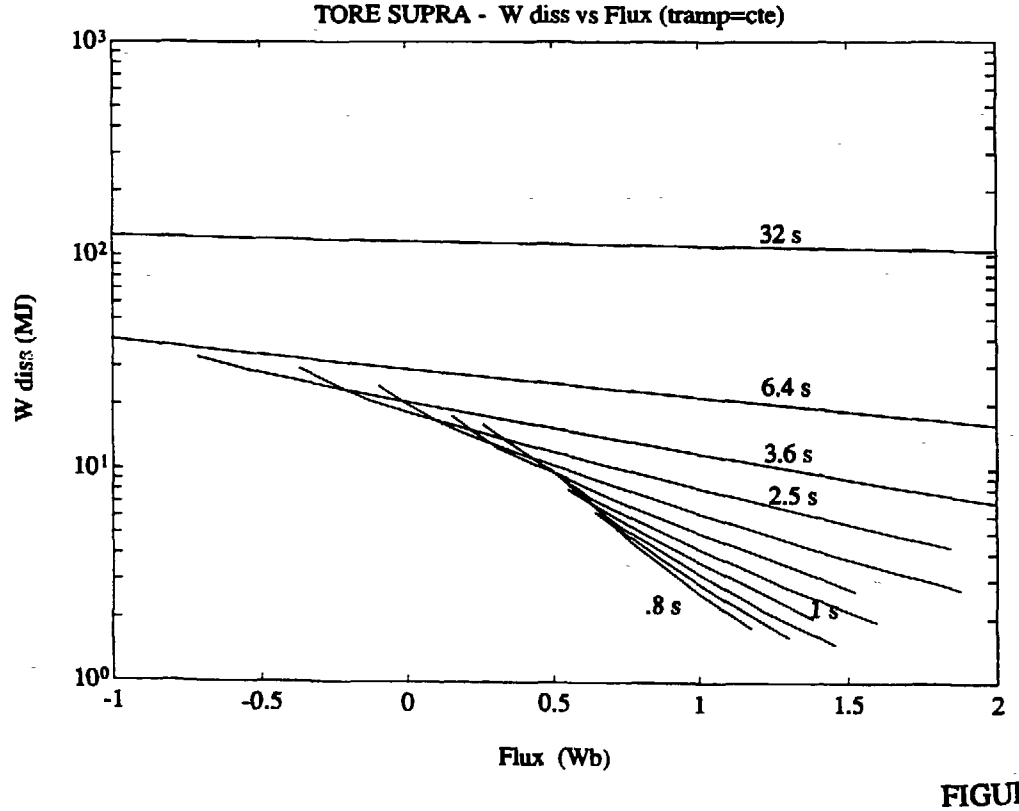
TORE SUPRA - W diss vs Flux (tramp=cte)
W diss (MJ)
Flux (Wb)
32 s
6.4 s
3.6 s
2.5 s
1 s
.8 s

FIGURE 5

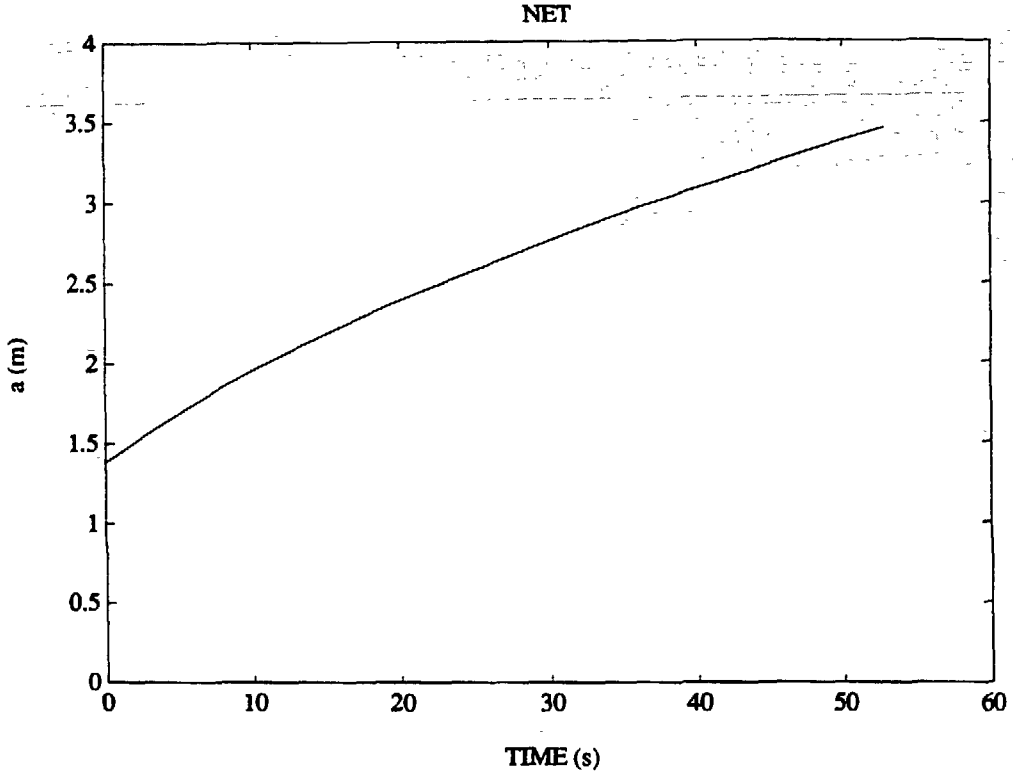
NET
a (m)
TIME (s)
0
0.5
1
1.5
2
2.5
3
3.5
4
0
10
20
30
40
50
60

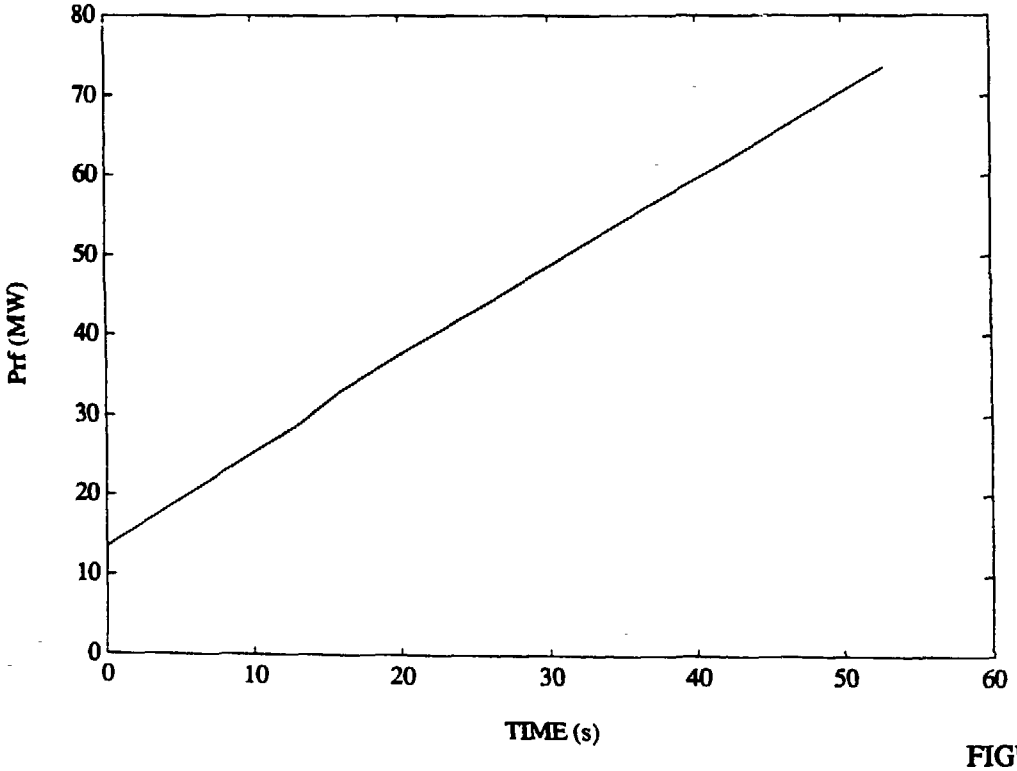
Prf (MW)
TIME (s)
0
10
20
30
40
50
60
70
80
0
10
20
30
40
50
60

FIGURE 6

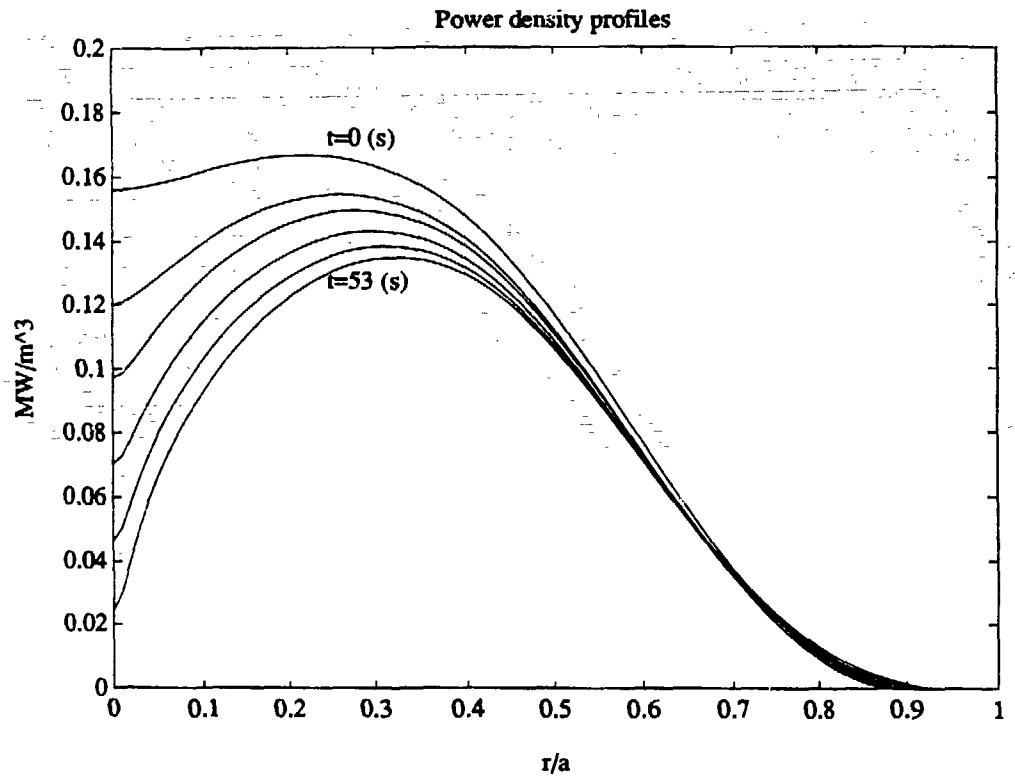
Power density profiles
t=0 (s)
t=53 (s)
MW/m^3
r/a
0.2
0.18
0.16
0.14
0.12
0.1
0.08
0.06
0.04
0.02
0
0.1
0.2
0.3
0.4
0.5
0.6
0.7
0.8
0.9
1

FIGURE 7

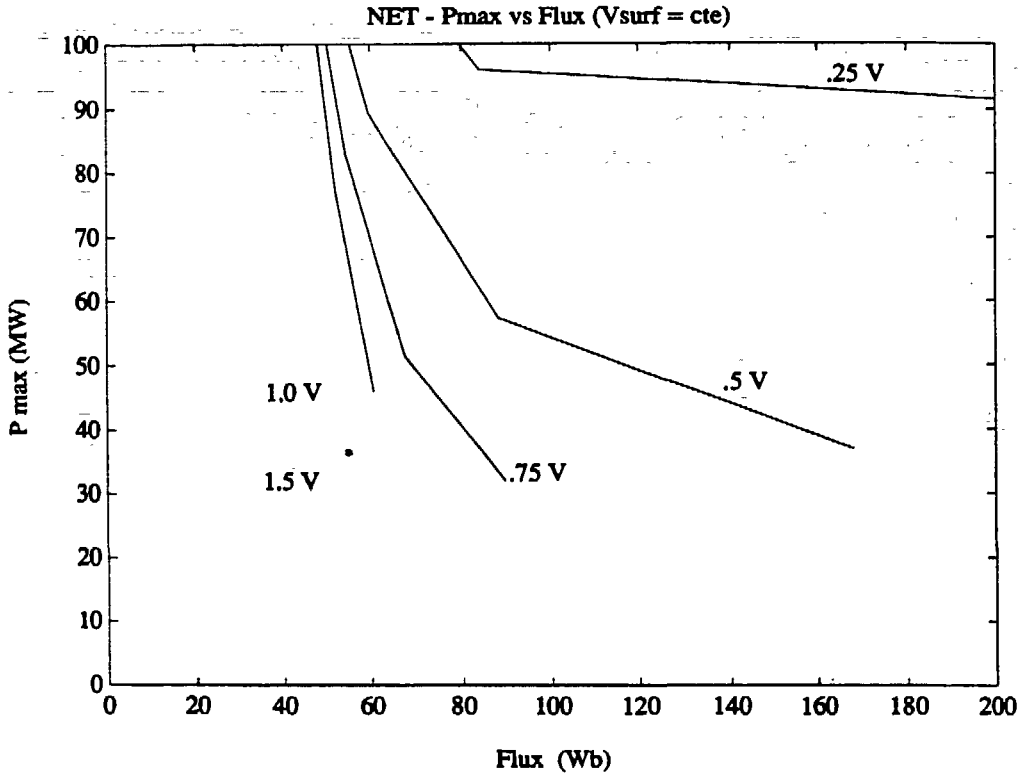
NET - Pmax vs Flux (Vsurf = cte)
P max (MW)
Flux (Wb)
.25 V
.5 V
.75 V
1.0 V
1.5 V
0
10
20
30
40
50
60
70
80
90
100
0
20
40
60
80
100
120
140
160
180
200

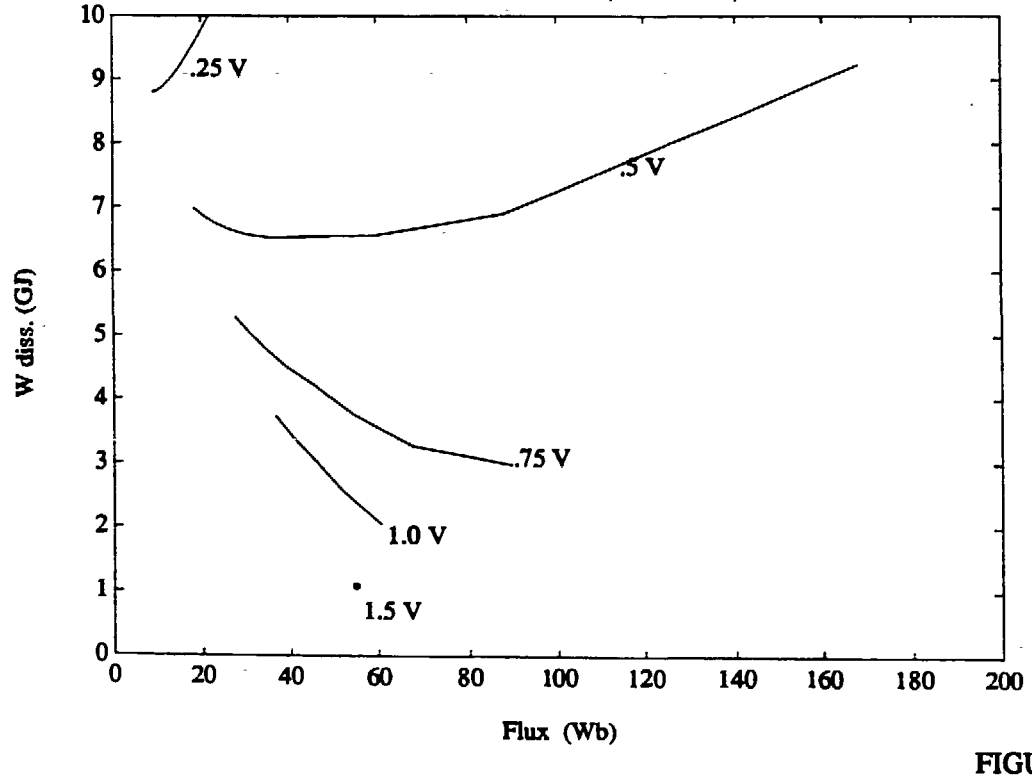
NET - W diss vs Flux (Vsurf = cte)
W diss. (GJ)
Flux (Wb)
.25 V
.5 V
.75 V
1.0 V
1.5 V
0
1
2
3
4
5
6
7
8
9
10
0
20
40
60
80
100
120
140
160
180
200

FIGURE 8

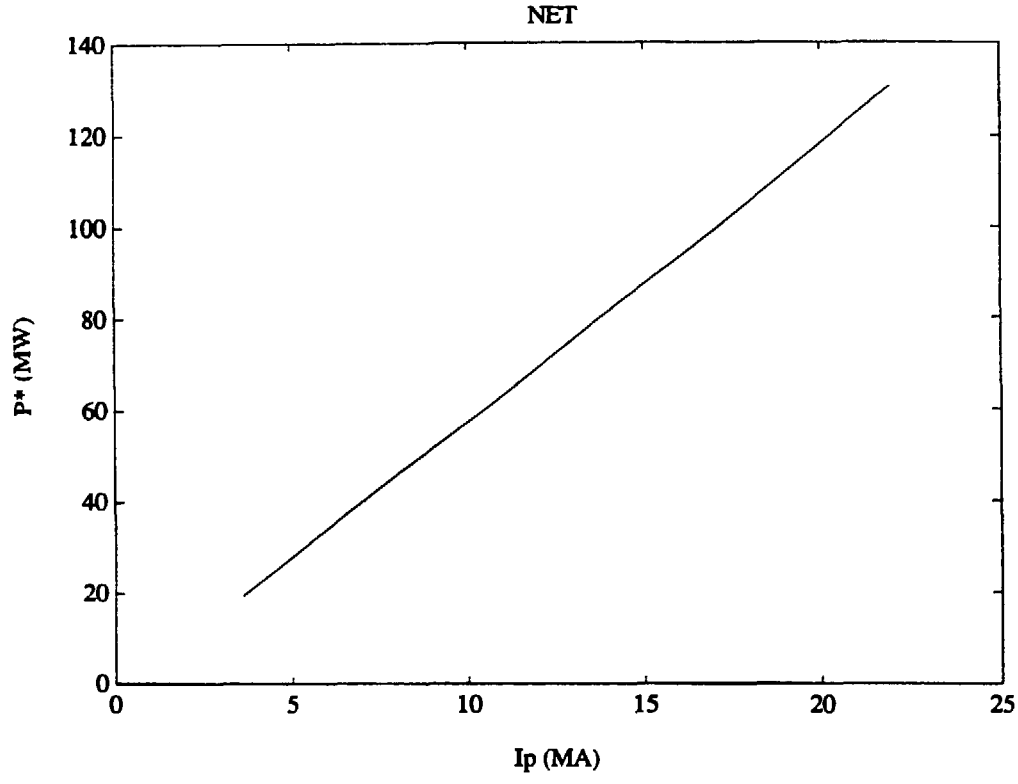
NET
P* (MW)
Ip (MA)
0
20
40
60
80
100
120
140
0
5
10
15
20
25

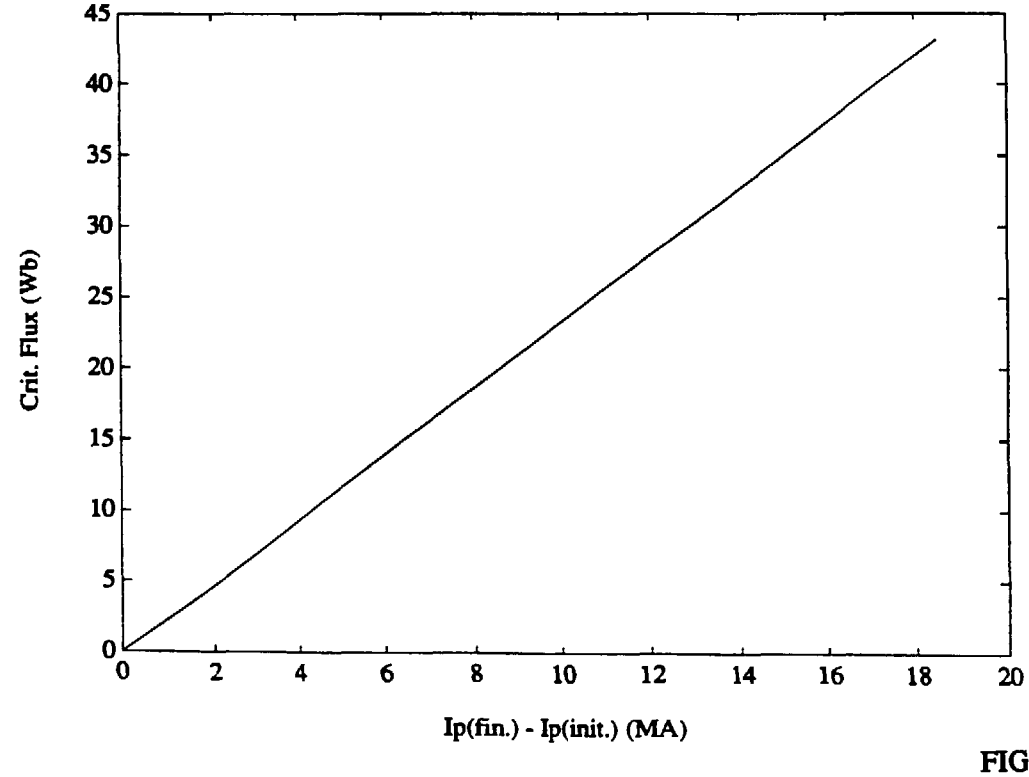
Crit. Flux (Wb)
Ip(fin.) - Ip(init.) (MA)
0
5
10
15
20
25
30
35
40
45
0
2
4
6
8
10
12
14
16
18
20

FIGURE 9

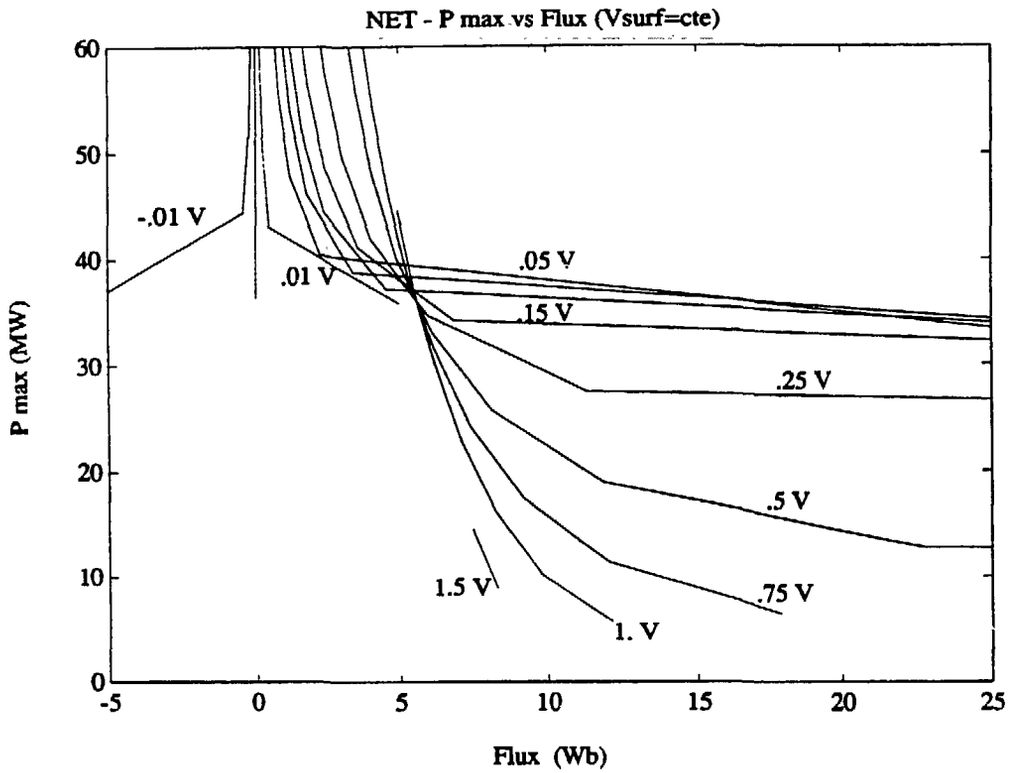
NET - P max vs Flux (Vsurf=cte)
P max (MW)
Flux (Wb)
-.01 V
.01 V
.05 V
.15 V
.25 V
.5 V
.75 V
1. V
1.5 V

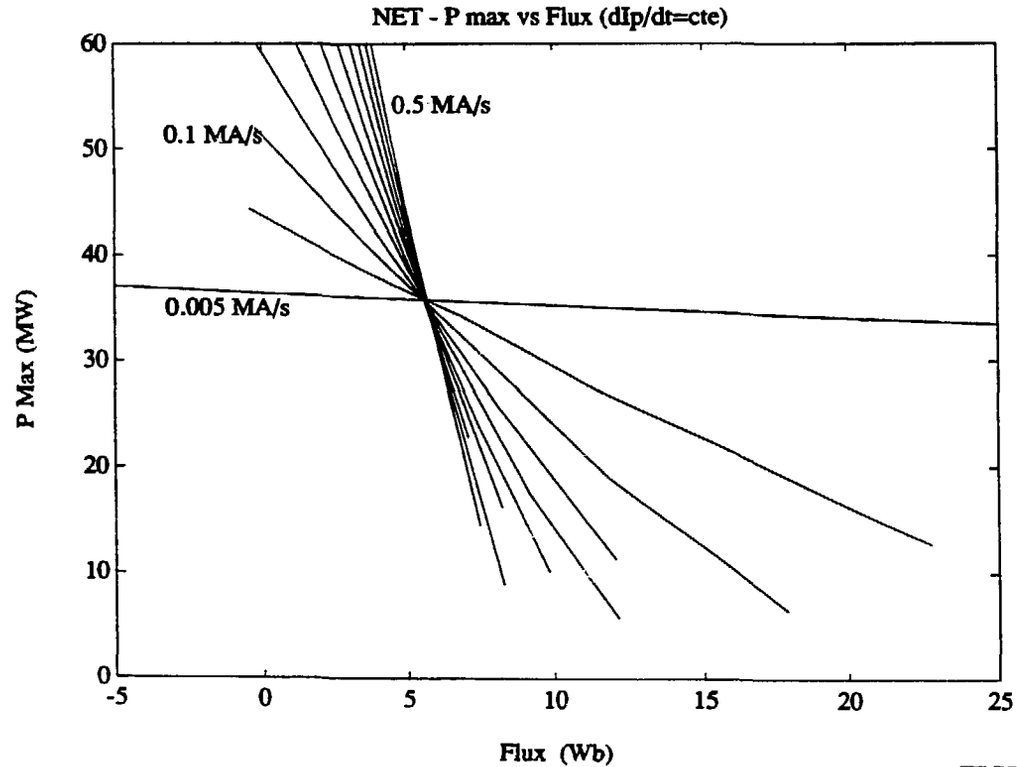
NET - P max vs Flux (dIp/dt=cte)
P Max (MW)
Flux (Wb)
0.5 MA/s
0.1 MA/s
0.005 MA/s

FIGURE 10

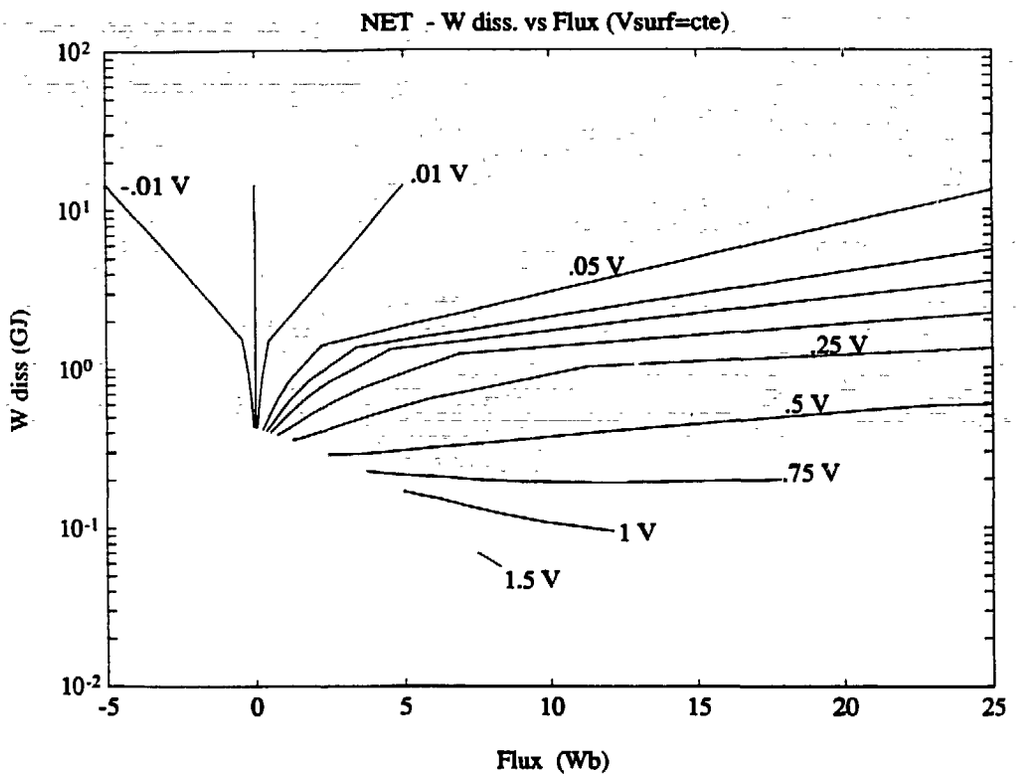
NET - W diss. vs Flux (Vsurf=cte)
W diss (GJ)
Flux (Wb)
-.01 V
.01 V
.05 V
.25 V
.5 V
.75 V
1 V
1.5 V

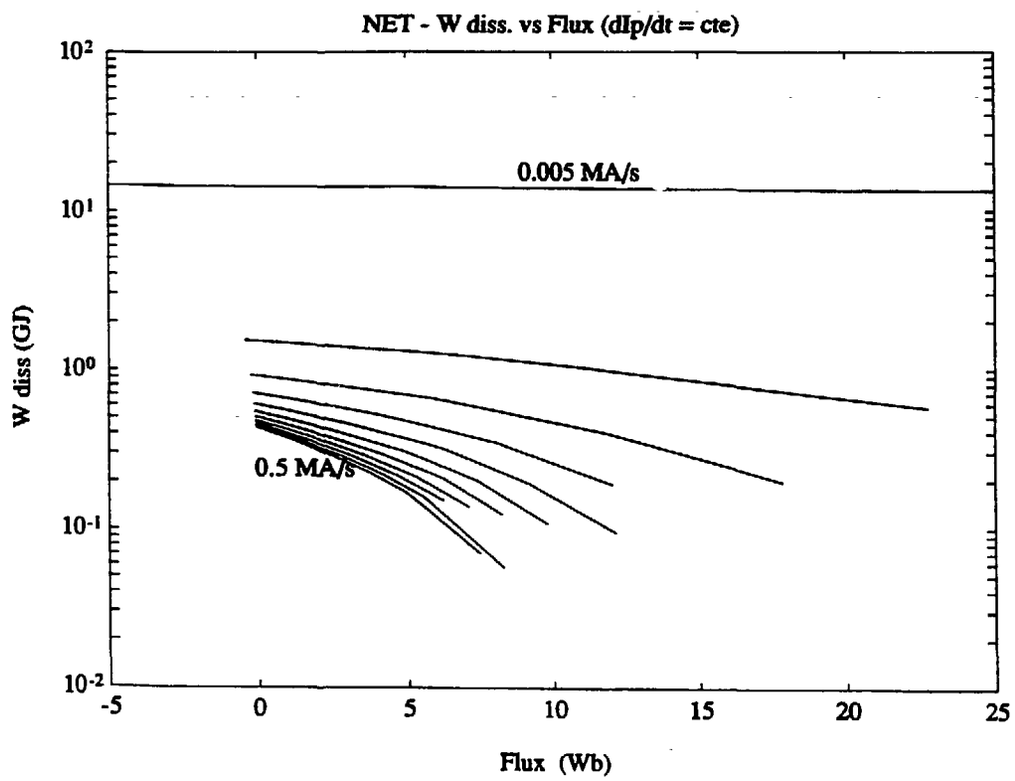
NET - W diss. vs Flux (dIp/dt = cte)
W diss (GJ)
Flux (Wb)
0.005 MA/s
0.5 MA/s

FIGURE 11

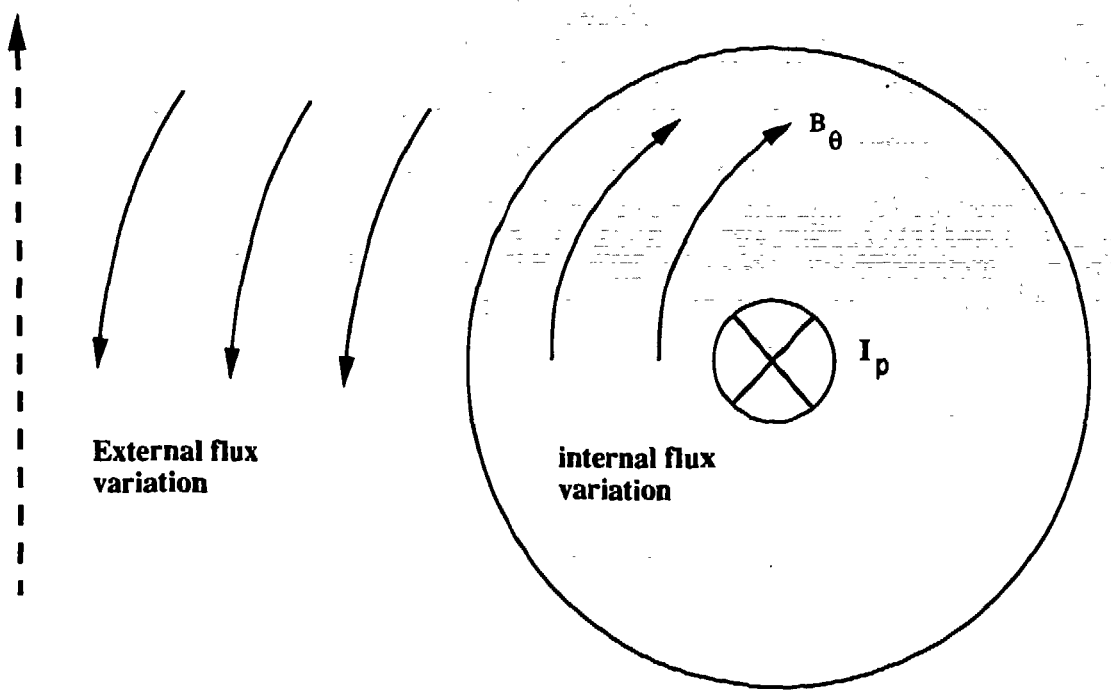
External flux
variation
B_θ
I_p
internal flux
variation

FIGURE 12